RESONANCES FROM STRONGLY-INTERACTING ELECTROWEAK SYMMETRY BREAKING SECTOR AT FUTURE $e^+ e^-$ COLLIDERS

M. Gintner[1], **I. Melo**[2]

Physics Dept.,University of Žilina, Veľký Diel, 010 26 Žilina, Slovakia

We study new strong resonances associated with the physics responsible for the strong electroweak symmetry breaking. We write down the lowest order effective chiral Lagrangians describing the couplings of these new resonances to the Standard Model fields and calculate signals for $I = J = 0$ S-resonances and for $I = J = 1$ ρ-resonances in the $WWt\bar{t}$ scattering in the process $e^+ e^- \rightarrow \nu\bar{\nu}t\bar{t}$ at the Next Linear Collider. We also find low-energy constraints on the ρ-resonance couplings to the top quark.

1 Introduction

One of the most important problems of today's particle physics is the mechanism of electroweak symmetry breaking (ESB). The mechanism of ESB is responsible for giving the W and Z bosons their masses. Despite some progress in the experimental limits on the Higgs mass [1], the ESB sector of the Standard Model (SM) is still rather weakly constrained by the experimental data and the physics behind the mechanism of ESB remains unknown.

There are two major scenarios for the solutions to this problem. The first scenario is a weakly-coupled electroweak symmetry breaking sector. Its simplest version is the light SM Higgs boson. More complicated alternatives of this scenario include supersymmetric theories. The second scenario is a strongly-coupled ESB sector. In this scenario the symmetry breaking is triggered by new non-perturbative strong forces. Typical representatives of this scenario are technicolor models built in analogy to chiral symmetry breaking in QCD. In this work we study some phenomenological consequences of strong ESB.

As a common feature of any plausible scenario, the originally massless W and Z gauge bosons become massive through the Higgs mechanism, by absorbing Goldstone bosons of the ESB sector. The Goldstone bosons are the inevitable product of a spontaneous symmetry breaking. When "eaten-up" by the W and Z bosons, the Goldstone bosons become their longitudinal components. A direct consequence of this fact is the Equivalence Theorem (ET): in the large energy limit ($E \gg M_W$) the interactions of the longitudinal W/Z's become equal to those of

---

[1]E-mail address: gintner@fel.utc.sk
[2]E-mail address: melo@fel.utc.sk

the ESB Goldstone bosons. Thus any collider process which involves the longitudinal weak gauge bosons can in principle give us an access to the interactions connected to the mechanism of ESB [2].

In QCD the spontaneous breaking of chiral symmetry gives rise to pions which are the bound states of quarks. At energies of a few hundred MeV we cannot see their substructure — we can only study QCD interactions through the $\pi\pi$ scattering amplitudes which are unitarized by some low-lying resonances such as $I = J = 1$ ρ-resonance or $I = 0, J = 1$ ω-resonance. We expect an analogical situation in the case of the strong ESB scenario. The strong ESB results in the appearance of massless Goldstone bosons — electroweak (EW) pions — which, just like QCD pions, are assumed to be bound states of some more fundamental strongly interacting objects (e.g. technifermions).

Since $V_L V_L$ ($V = W, Z$) scattering amplitudes start to violate unitarity at 1-3 TeV range we expect new strongly interacting ESB resonances to appear at or below this scale. We will not be able to see the substructure of these new resonances and EW pions at the Large Hadron Colider (LHC) and at the Next Linear Collider (NLC) operating at 1-3 TeV range, but the question is if we can distinguish at least the resonances themselves and measure their masses and couplings.

A lot of attention has been devoted to the testing of the strongly-interacting scenario in the longitudinal vector boson scattering $V_L V_L \to V_L V_L$ [3]. The studies concentrated on signatures of either a new $I = J = 1$ ρ-resonance or a new $I = J = 0$ S-resonance (parameters of the S-resonance can be tuned to immitate the SM Higgs boson — SM-like S-resonance) at either the NLC or the LHC. The results have shown that it will be possible to establish the presence of strong ESB at the LHC and the NLC and that, to a degree, it will be possible to distinguish new strong resonances [2].

Another potentially powerful process for the study of strong ESB is the scattering of longitudinal vector bosons to top quarks, $V_L V_L \to t\bar{t}$. Its main appeal is in the possibility to test whether the extraordinarily large top quark mass is generated by the same new strong interactions which are responsible for ESB, or by yet additional new strong interactions introduced just for that sake. In the former case (represented, e.g., by the extended technicolor theories [4]) we expect the top quark to couple significantly to the resonances which unitarize $V_L V_L \to V_L V_L$ scattering [5, 6]. This could lead to significant event rates in $V_L V_L \to t\bar{t}$. In the latter case, when the mechanism of the top mass generation is different from the W mass generation (as in topcolor-assisted technicolor models [4]), we expect that the top quark does not couple significantly to the new resonances of the strong ESB sector. This would imply that the new resonances observed in the $V_L V_L \to V_L V_L$ channel are suppressed in the $V_L V_L \to t\bar{t}$ channel [2, 5].

When studying the $V_L V_L \to t\bar{t}$ process, we can make use of another unique property of the top quark. Unlike all the other known quarks the top quark decays so rapidly that the information about its spin is transferred directly to the final state with negligible hadronization uncertainties. This raises an interesting possibility to measure polarized cross sections in $V_L V_L \to t\bar{t}$ and use this information to distinguish between S- and ρ resonances which contribute to different helicity combinations of the top quarks [2, 5].

For these reasons the $V_L V_L \to t\bar{t}$ process at the NLC has recently attracted growing interest. There have been studies within the SM [7–9], within the Higgsless SM below the scale of new physics (no-resonance model) [6, 10], and also within models above the scale of a new S-resonance and ρ-resonance [2, 5, 11, 12].

In this work we study the new S- and ρ-resonances in the process $W_L W_L \to t\bar{t}$ which is

being considered as a subprocess of $e^+e^- \to \nu\bar{\nu}t\bar{t}$ at the NLC with the CM energy of 1.5 TeV and 2 TeV. Three cases, the no-resonance, the S-resonance, and the ρ-resonance are considered with various values of parameters. We show the importance of low energy constraints for ρ-resonance signals at NLC. We calculate total and differential cross sections with polarized $(\mathrm{anti}-)\mathrm{top}$ quarks in the final state using the Effective-W Approximation and considering longitudinal weak gauge bosons only. The number of events obtained is for the assumed integrated luminosity of 200 fb^{-1}.

This paper is organized as follows. In Section 2 we introduce the lowest order effective chiral Lagrangians describing models with no resonance, S-resonance, and ρ-resonance. The Lagrangians describe interactions of these resonances with EW pions, gauge fields, and top quarks. In Subsection 2.1 we discuss existing constraints on the parameters of the ρ Lagrangian. Our calculations and results obtained for the models under consideration are presented in Section 3. Finally, our conclusions can be found in Section 4.

2   No- ,S- and ρ-resonance models

Due to our ignorance of details of new strong physics behind ESB the most convenient approach to the analysis of its possible consequences is the effective field theory framework. Within this framework a model-independent analysis of the strong ESB mechanism can be performed. Our ignorance of the full theory will be reflected in our inability to calculate values of free parameters that appear in an effective Lagrangian. These free parameters parameterize all possible new physics which respects the given low-energy theory. They will have to be obtained from experiment.

In this approach, if energy available is below the threshold of new resonances production, one starts with EW pions as the only particles in the spectrum which are subject to new strong interactions. The Lagrangian of EW pions is the familiar nonlinear σ-model based on global $SU(2)_L \times SU(2)_R$ spontaneously broken down to $SU(2)_V$ custodial or isospin symmetry. This symmetry breaking pattern is supported by the relation $M_W/M_Z = \cos\theta_W$ which is satisfied to high accuracy.

If we assume to have enough energy to produce a new resonance it must be added to the set of building elements of the effective Lagrangian. In our work beside the no-resonance case we also assume the production of either the S-resonance or ρ-resonance. They are added to the Lagrangian respecting chiral $SU(2)_L \times SU(2)_R$ symmetry. For S-resonance it is a straightforward procedure, for ρ-resonance one can follow either Weinberg [13] or hidden symmetry approach [14]. The gauge interactions of the SM are introduced by requiring the S and ρ Lagrangians to be gauge invariant under $SU(2)_L \times U(1)_Y$.

Let us begin with the no-resonance Lagrangian. The $SU(2)_L \times U(1)_Y$ gauged non-renormalizable effective Lagrangian responsible for the low energy interactions of the EW pions is given by

$$\mathcal{L}_0 = \frac{v^2}{4}\mathrm{Tr}(D_\mu U^\dagger D^\mu U) + \mathcal{L}_{kin}(W, Y) \tag{1}$$

where $U = \exp(2i\vec{\pi}\vec{\tau}/v)$ with $v = 246$ GeV, $\vec{\pi}$ is the isospin triplet of the EW pions, and τ^a $(a = 1, 2, 3)$ are the $SU(2)$ group generators with the normalization $\mathrm{Tr}(\tau^a\tau^b) = \delta^{ab}/2$.

$\mathcal{L}_{kin}(W, Y)$ is the kinetic energy term of the $SU(2)_L$ gauge fields, W_μ^a ($a = 1, 2, 3$), and the $U(1)_Y$ gauge field, Y_μ. The covariant derivative $D_\mu U$ is defined as follows

$$D_\mu U = \partial_\mu U - iU\mathcal{L}_\mu + i\mathcal{R}_\mu U \tag{2}$$

where $\mathcal{L}_\mu = g\vec{W}_\mu\vec{\tau}$ and $\mathcal{R}_\mu = g'Y_\mu\tau^3$.

In this model the interactions of EW pions with fermions are described by the following Lagrangian

$$
\begin{aligned}
\mathcal{L}_0^f \;=\; & \bar{\psi}_L i\gamma^\mu \big[\partial_\mu + ig\vec{W}_\mu\vec{\tau} + ig'\tfrac{1}{2}(B - L)Y_\mu\big]\psi_L \\
& + \bar{\psi}_R i\gamma^\mu \big\{\partial_\mu + ig'[\tau^3 + \tfrac{1}{2}(B - L)]Y_\mu\big\}\psi_R \\
& - (\bar{\psi}_L U^\dagger M\psi_R + \text{h.c.})
\end{aligned}
\tag{3}
$$

where the ψ denotes fermion field doublet, (t, b), the $B - L$ is the baryon minus lepton number operator, and the $M = \text{diag}(m_t, m_b)$ is the fermion doublet mass matrix.

The gauged S-resonance model can be described by the following leading order effective Lagrangian

$$\mathcal{L}_S = \mathcal{L}_0 + \frac{1}{2}M_S^2 S^2 + g'''\frac{v}{2}\text{Tr}(D_\mu U^\dagger D^\mu U)S + \mathcal{L}_{kin}(S) \tag{4}$$

where $\mathcal{L}_0$ is given by (1), the $\mathcal{L}_{kin}(S)$ is the kinetic energy term of the S-resonance, the S denotes the scalar ($I = J = 0$) resonance field, the M_S is its mass. The g''' and M_S are free parameters.

To include the interactions with fermions we have to add

$$\mathcal{L}_S^f = \mathcal{L}_0^f - (\frac{\alpha}{v}\bar{\psi}_L U^\dagger M\psi_R S + \text{h.c.}) \tag{5}$$

where $\mathcal{L}_0^f$ is given by (3), and α is a free parameter.

The gauged ρ-resonance model is given by

$$\mathcal{L}_\rho = \mathcal{L}_0 - a\frac{v^2}{4}\text{Tr}(\mathcal{V}_\mu \mathcal{V}^\mu) + \mathcal{L}_{kin}(V) \tag{6}$$

where $\mathcal{L}_0$ is given by (1), the $\mathcal{L}_{kin}(V)$ is the kinetic energy term of the ρ-resonance, and

$$\mathcal{V}_\mu = \alpha_\mu^\parallel + iV_\mu + \frac{i}{2}(\xi^\dagger \mathcal{R}_\mu\xi + \xi\mathcal{L}_\mu\xi^\dagger) \tag{7}$$

where $\xi = \exp(i\vec{\pi}\vec{\tau}/v)$, $\alpha_\mu^\parallel = (\xi^\dagger\partial_\mu\xi + \xi\partial_\mu\xi^\dagger)/2$, and the $V_\mu = g''\vec{V}_\mu\vec{\tau}$ denotes the vector ($I = J = 1$) ρ-resonance field. The a and the g'' are free parameters.

The fermionic part of the ρ-resonance model is described as follows

$$
\begin{aligned}
\mathcal{L}_\rho^f \;=\; & b_1\bar{\psi}_L\xi^\dagger i\gamma^\mu \big[\partial_\mu - ig''\vec{V}_\mu\vec{\tau} + i\tfrac{1}{2}(B - L)Y_\mu\big]\xi\psi_L \\
& + b_2\bar{\psi}_R P\xi i\gamma^\mu \big[\partial_\mu - ig''\vec{V}_\mu\vec{\tau} + i\tfrac{1}{2}(B - L)Y_\mu\big]\xi^\dagger P\psi_R
\end{aligned}
\tag{8}
$$

where the b_1, b_2 are free parameters, and $P = \text{diag}(1, 0)$.

This Lagrangian is $SU(2)_L \times U(1)_Y$ gauge invariant. However, introduction of gauge fields broke the original $SU(2)_L \times SU(2)_R$ chiral invariance, namely by the terms with the weak hypercharge. More precisely, it is the custodial $SU(2)_V$ that got broken by the Y_μ terms. The custodial symmetry is also broken by the top-bottom quark mass splitting in the fermion mass term. These two particular breakings of the custodial symmetry also occur in the SM. The third custodial symmetry breaking originates in the projection matrix P in the coupling of the ρ to the ψ_R. The P matrix ensures that the ρ only couples to the right-handed top quark but not to the right-handed bottom quark (to avoid constraints on the ρ couplings from the $Zb\bar{b}$ vertex), which spoils the custodial symmetry in much the same fashion as does the top-bottom mass splitting.

The difference between our ρ-resonance Lagrangian and the BESS model of Ref. [15] is that in the BESS model $b_2 = 0$ and b_1 is assumed to be universal for all fermion generations, while here we assume coupling constants b_1, b_2 to be specific (and possibly large) for the third generation of quarks.

2.1 Constraints on the parameters of the ρ Lagrangian

There are four new parameters in the ρ Lagrangian: couplings a, g'', b_1, b_2. Since $M_{\rho_T} = av^2 g''^2/4$ the coupling a can be traded for the ρ mass. We do not have any experimental constraints on M_{ρ_T} (the theoretical expectation is that it should be around $1 - 3$ TeV scale). We do, however, have constraints on g'', b_1 and b_2. These are due to the corrections that g'', b_1 and b_2 induce in the SM couplings of the Z and the W to fermions at low energies (~ 90 GeV) when the ρ-resonance is integrated-out from the particle spectrum. This leads to corrections to ϵ parameters which conveniently parameterize new physics effects [16]. The BESS model studies [17] have shown that g'' corrects ϵ_3 by $\delta\epsilon_3 = g^2/(4g''^2)$, which implies for our model

$$g'' \stackrel{>}{\sim} 10. \tag{9}$$

We will now derive constraints on the b_1 and b_2 parameters which are specific to our model. We find the low-energy couplings of the Z and the W to fermions by taking $M_{\rho_T} \to \infty$, which is accomplished by $a \to \infty$ while keeping g'' fixed, as in the BESS model studies [17]. In this limit the equation of motion for the V_μ field ($\partial \mathcal{L}_\rho/\partial V_\mu = 0$) has the solution $V_\mu = -(\mathcal{L}_\mu + \mathcal{R}_\mu)/2$. When we substitute this solution in the fermion Lagrangian in (8) and follow usual steps, we eventually get for the low-energy Z and W couplings to the top and bottom quarks [3]:

$$
\begin{aligned}
\mathcal{L}_f &= \frac{g}{\sqrt{2}}(-1 + \frac{b_1}{2})\, \bar{t}_L \gamma^\mu b_L W_\mu^+ + h.c. \\
&+ \frac{g}{2c_\theta}(1 - \frac{4}{3}s_\theta^2 - \frac{b_1}{2})\, \bar{t}_L \gamma^\mu t_L Z_\mu + \frac{g}{2c_\theta}(-\frac{4}{3}s_\theta^2 + \frac{b_2}{2})\, \bar{t}_R \gamma^\mu t_R Z_\mu \\
&+ \frac{g}{c_\theta}(-\frac{1}{2} + \frac{1}{3}s_\theta^2 + \frac{b_1}{4})\, \bar{b}_L \gamma^\mu b_L Z_\mu + \frac{g}{c_\theta}\frac{1}{3}s_\theta^2\, \bar{b}_R \gamma^\mu b_R Z_\mu,
\end{aligned}
\tag{10}
$$

where $c_\theta, s_\theta = \cos\theta_W, \sin\theta_W$, respectively. There is no modification of the Z or W couplings to leptons and the first and second generation quarks. Note that b_1 modifies the Wtb, Ztt and Zbb couplings, while b_2, due to the matrix P in the $V_\mu \psi_R \psi_R$ coupling in (8) modifies only Ztt coupling (b_2 thus escapes the constraint from the Zbb coupling).

---

[3] These couplings are also modified by the small terms $\sim g^2/g''^2$ which we neglect here for simplicity.

The constraint on b_1 follows from the Zbb vertex. Using the definition of ϵ_b [16] and Eq. (10) we find a tree level contribution to ϵ_b parameter, $\delta\epsilon_b = -b_1/2$. We then use the experimental value of ϵ_b to constrain the theoretical prediction at 2σ level [18]:

$$-8.32 \times 10^{-3} \leq \epsilon_b^{SM} + \delta\epsilon_b \leq -0.88 \times 10^{-3}, \tag{11}$$

where $\epsilon_b^{SM} = -6.5 \times 10^{-3}$. The corresponding limit is

$$|b_1| \overset{<}{\sim} 0.01, \tag{12}$$

which is a relatively strong constraint (for this reason and also for simplicity we set b_1 equal to zero in our calculations). As noted above, b_1 also modifies the Wt_Lb_L coupling which affects $b \to s\gamma$ rate but this does not place significant constraint on b_1 [12].

For b_2, which modifies only Ztt coupling, there is no tree level contribution to ϵ parameters. There is, however, an important one-loop contribution to ϵ_1 from the modified Ztt coupling. It comes from the diagrams such as, e.g., $t\bar{t}$ loop in the Z boson self-energy, famous for its m_t^2 dependence which led to the successful prediction of the top quark mass before the top quark was actually discovered. The analysis of Ref. [18], when applied to (10), yields

$$\delta\epsilon_1 = (b_2 + 2b_1)\frac{3m_t^2 G_F}{2\sqrt{2}\pi^2}\ln\frac{\Lambda}{m_t}, \tag{13}$$

where Λ is the cut-off scale of the divergent one-loop graphs. We now use the experimental value of ϵ_1 to constrain the theoretical prediction at 2σ level [18]:

$$1.5 \times 10^{-3} \leq \epsilon_1^{SM} + \delta\epsilon_1 \leq 5.9 \times 10^{-3}, \tag{14}$$

where $\epsilon_1^{SM} = 3.32 \times 10^{-3}$. This implies (for $b_1 = 0$)

$$-0.03 \overset{<}{\sim} b_2 \overset{<}{\sim} 0.04. \tag{15}$$

Note that Λ is not well defined (we use $\Lambda = 1$ TeV) and further uncertainties come from the possible contributions to ϵ parameters from the higher order operators in the chiral perturbation expansion (e.g., dim 6 operators as in Ref. [20]). For these reasons we will use besides $b_2 = 0.04$ also $b_2 = 0.08$ in our calculations.

Finally, we note that in the model of Ref. [12], in contrast to our model, the bound on the the right-handed coupling is much stronger than the bound of Eq. 15 and the bound on the left-handed coupling is much weaker than the bound given by (12). We avoided the stronger constraint on the right-handed coupling by introducing the P matrix but we do not see a way to avoid the constraint on the left-handed coupling given by (12).

3 Signals from the S- and the ρ-resonances at the NLC

The question is if the ρ coupling constants which respect constraints of Sec. 2.1 can generate significant signals in the $W_LW_L \to t\bar{t}$ scattering at the NLC. Here we consider this scattering as a subprocess of the process $e^+e^- \to \nu\bar{\nu}t\bar{t}$, see Fig. 1.

We have chosen to calculate signals for three ρ-resonances of the same mass $M_{\rho_T} = 1$ TeV but different couplings and widths Γ_{ρ_T}, summarized in Table 1. For comparison we also calculate
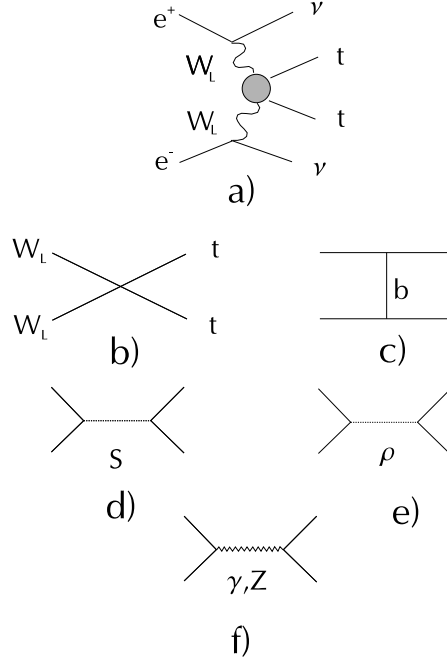
Fig. 1. Feynman diagrams for a) $e^+e^- \to \nu\bar{\nu}t\bar{t}$, b-f) $W_L W_L \to t\bar{t}$

signals from two S-resonances — 800 GeV SM-like Higgs boson with the width $\Gamma_H = 285$ GeV ($g''' = \alpha = 1$) and the nonstandard 800 GeV S-resonance with the width $\Gamma_S = 158$ GeV ($g''' = 0.7, \alpha = 1$) — and from the no-resonance model.

To calculate cross sections of the process $e^+e^- \to \nu\bar{\nu}t\bar{t}$ we used Effective-W Approximation (EWA) [19] in which one convolutes the cross section for the subprocess $W_L W_L \to t\bar{t}$ with the corresponding distribution functions of the W_L boson. For the EWA to be valid the invariant energy scales of the process should be much larger than the W mass. Since the distribution function for longitudinal W-bosons is largely independent of the W beam energies the EWA describes more accurately W_L contributions than contributions of transverse W-bosons. Fortunately, sensitivity of W_T channels to the ESB sector is much weaker than sensitivity of W_L channels. Therefore to extract the signal of new physics without having the transverse W

	M_{ρ_T} (TeV)	b_1	b_2	g''	Γ_{ρ_T} (GeV)
ρ_1	1	0	0.04	15	4.99
ρ_2	1	0	0.08	10	9.42
ρ_3	1	0	0.04	40	21.66

Table 1: Parameters of the three ρ-resonances. Γ_{ρ_T} is uniquely defined by M_{ρ_T} and the three coupling constants.
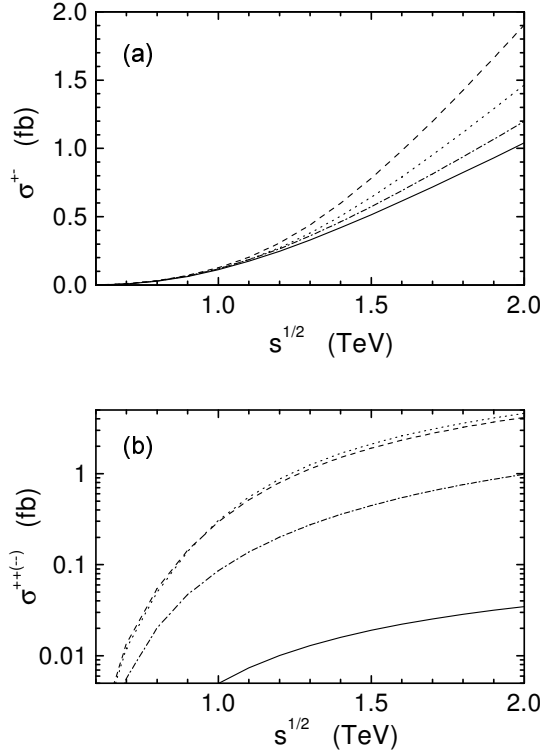
Fig. 2. Helicity cross sections for $e^+e^- \rightarrow \nu\bar{\nu}t\bar{t}$ as a function of CM energy: (a) σ^{+-} for the three ρ-resonances of Table 1: ρ_1 (dotted line), ρ_2 (dashed line), ρ_3 (dash-dotted line). The solid line is for both the S-resonance and the no-resonance signal; (b) σ^{++} ($= \sigma^{--}$) for the nonstandard 800 GeV S-resonance with $\Gamma_S = 158$ GeV (dotted line), the 800 GeV SM-like Higgs boson (dashed line), all ρ-resonances and the no-resonance model (dash-dotted line), the 100 GeV SM Higgs (solid line).

contributions calculated the following quantity can be used [12]

$$\sigma_{\text{new physics}} - \sigma_{SM}(M_H = 100\,\text{GeV}) \tag{16}$$

Here the transverse W contributions are expected to subtract each other. Thus the difference (16) should be a good estimate of what we would get if much more complete calculations of the studied process were performed.

To calculate the subprocess cross sections we used the ET theorem according to which we replaced W_L boson with the corresponding EW pion π. The subprocess diagrams are shown in Figs. 1b – 1f. The main contribution comes from the diagrams 1b – 1e, while the contribution of the diagram 1f is small. We note that the helicity cross sections $\sigma^{++} = \sigma^{--}$ (the signs refer to helicities of the t and $\bar{t}$, respectively) receive their contributions mainly from the diagrams 1b and 1d, σ^{+-} mainly from 1c and 1e while σ^{-+} is negligible.

We show the results of our calculations in Fig. 2. Fig. 2a shows the total cross section σ^{+-} for the process $e^+e^- \rightarrow \nu\bar{\nu}t\bar{t}$ in femtobarns as a function of the CM energy $\sqrt{s}$ of the NLC. The

signals from the ρ resonances rise above the solid line which represents both the S-resonances and the no-resonance model at the same time (they have approximately the same σ^{+-}). The best signal comes from the ρ-resonance with the width $\Gamma_{\rho_T} = 9.42$ GeV ($b_2 = 0.08$, $g'' = 10$) — for $\sqrt{s} = 1.5$ TeV and $\sqrt{s} = 2$ TeV we get cross sections 0.8 fb and 1.9 fb, respectively. Assuming integrated luminosity $L = 200$ fb^{-1} we get for the ρ-resonance 160 events at $\sqrt{s} = 1.5$ TeV and 380 events at $\sqrt{s} = 2$ TeV. For S-resonances and the no-resonance model we get 102 events at $\sqrt{s} = 1.5$ TeV and 208 events at $\sqrt{s} = 2$ TeV. We note that the only cut performed on data was the cut on the invariant mass of the $t\bar{t}$ pair $m_{tt} > 500$ GeV. Further cuts are needed to reduce the backgrounds which are not treated here. Following previous studies [12] we estimate that the efficiency of these cuts for the signal is about $\epsilon_{cut} = 80$ % and that the remaining events will be fully reconstructed (including b-tagging) with the efficiency of about $\epsilon_{rec} = 30$ % [5]. Hence, for the final event numbers $N_f = N\epsilon_{cut}\epsilon_{rec}$. For the ρ-resonance we thus finally get 38 (91) events at 1.5 TeV (2 TeV), and for S-resonances and the no-resonance case 24 (50) events at 1.5 TeV (2 TeV).

In Fig. 2b we show the total cross section $\sigma^{++} = \sigma^{--}$ for the process $e^+e^- \to \nu\bar{\nu}t\bar{t}$ in femtobarns as a function of the CM energy $\sqrt{s}$. In this case the S-resonances dominate: for the SM-like Higgs we get $\sigma^{++} + \sigma^{--} = 3.8$ (8.3) fb at $\sqrt{s} = 1.5$ (2) TeV, while for the ρ-resonances and the no-resonance model we get the same results $\sigma^{++} + \sigma^{--} = 0.9$ (1.8) fb at $\sqrt{s} = 1.5$ (2) TeV. After the cuts and the reconstruction we get for the SM-like Higgs 182 (398) events at 1.5 (2) TeV and for the ρ- and the no-resonance case 43 (86) events at 1.5 (2) TeV.

Differential cross sections for $e^+e^- \to \nu\bar{\nu}t\bar{t}$ as a function of the invariant mass m_{tt} at $\sqrt{s} = 1.5$ TeV are shown for $(+-)$ helicity combination in Fig. 3a and for $(++)$ helicity combination in Fig. 3b. The measurement of these differential cross sections could provide the resonance mass if the resonance has a well defined peak with sufficient number of events contributing to the peak. For ρ_2 (solid line in Fig. 3a), we get 37 events in the peak before the cuts and reconstruction, assuming integrated luminosity $L = 200$ fb^{-1}.

4 Conclusions

We have studied the new strong resonances associated with the physics responsible for the strong electroweak symmetry breaking and signals of these resonances in the process $e^+e^- \to \nu\bar{\nu}t\bar{t}$. We have provided the comprehensive treatment of the ρ Lagrangian including the low-energy constraints on its parameters. The analysis presented in this work shows that the total signal from the ρ-resonance summed through all helicity channels at the energy of 1.5 TeV and the integrated luminosity of 200 fb^{-1} is 81 events after the cuts and reconstruction. The corresponding numbers for 800 GeV SM-like Higgs is 206 events and for the no-resonance case 67 events. The SM-like 800 GeV Higgs (and heavy S-resonances in general) is thus well separated from the ρ-resonance and the no-resonance cases. To distinguish the ρ-resonance signal from the no-resonance one and to confirm the spin of the S-resonance it is very useful to study individual helicity channels and distributions in invariant mass m_{tt}. The ρ-resonance contributes mainly to the helicity cross section σ^{+-} for the process $e^+e^- \to \nu\bar{\nu}t\bar{t}$, while the S-resonance contributes mainly to the cross section σ^{++}. This underlines the importance of the measurement of the top quark helicity (see Ref. [5] for more on this). Another way to improve on signals is to go to the CM energy of 2 TeV.
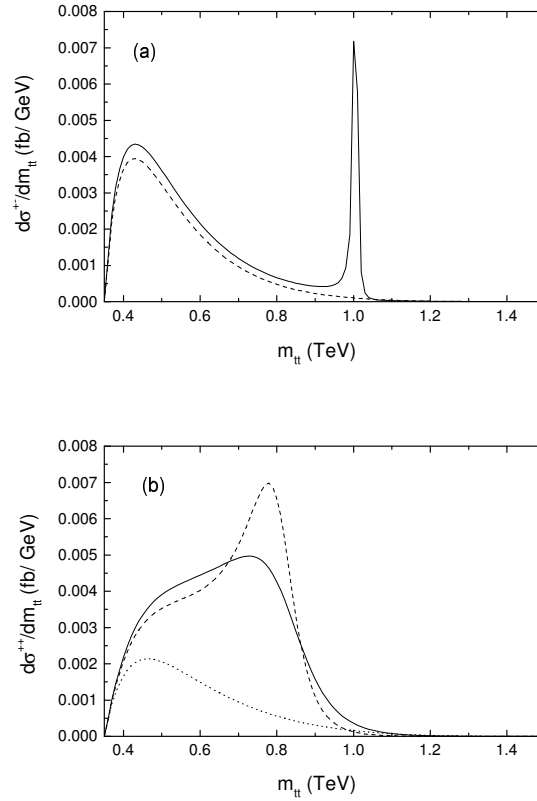
Fig. 3. Differential cross sections for $e^+e^- \to \nu\bar{\nu}t\bar{t}$ as a function of the invariant mass m_{tt} at $\sqrt{s} = 1.5$ TeV: (a) $\frac{d\sigma^{+-}}{dm_{tt}}$ for ρ_2 (solid line), the S-resonances and the no-resonance case (dashed line); (b) $\frac{d\sigma^{++}}{dm_{tt}}$ for the 800 GeV SM-like Higgs boson (solid line), the 800 GeV nonstandard S-resonance with $\Gamma_S = 158$ GeV (dashed line), all ρ-resonances and the no-resonance model (dotted line).

The significance of the presented signals depends on the backgrounds. We would like to note that the situation regarding this important issue is somewhat confusing, with, e.g., Ref. [12] reporting the SM background cross section value of 0.21 fb at 1.5 TeV and Ref. [10] the value of 1.8 fb at 1.5 TeV. Clearly, more dedicated effort is required to settle this issue.

References

[1] M. Swartz: *Plenary talk presented at the XIX International Symposium on Lepton and Photon Inter-actions at High Energies, Stanford University*, Aug. 9-14, 1999, [hep-ex/9912026]; *L3 Collaboration, presentation at LEPC* CERN, November 1999,
    [http://l3www.cern.ch/conferences/talks99.html]

[2] T.L. Barklow et al.: *Strong coupling Electroweak Symmetry Breaking*, Working Group Summary

Report from the 1996 DPF/DPB Summer Study New Directions for High Energy Physics Snowmass, Colorado, June 25–July 12, 1996, `[hep-ph/9704217]`

[3] M. Golden, T. Han, G. Valencia: *Report contributed to ESB & BSM Book* (Eds. by T. Barklow, S. Dawson, H. Haber, J. Siegrist). `[hep-ph/9511206]`; J. Bagger et al: *Phys. Rev. D* **49** (1994) 1246 `[hep-ph/9306256]`; R. Casalbuoni et al: *Z. Phys. C* **60** (1993) 315 ; See also Ref. [2] and references therein

[4] For a review of technicolor/extended technicolor theories and topcolor-assisted technicolor theories see K. Lane "Technicolor 2000", `[hep-ph/0007304]`

[5] E.R. Morales, M.E. Peskin: *Proceedings of the International Workshop on Linear Colliders*, Sitges, Barcelona, Spain, 28 April – 5 May, 1999, `[hep-ph/9909383]`

[6] T. Lee: *Phys. Lett.* **B 315** (1993), 392.

[7] R. P. Kauffman: *Phys. Rev.* **D41** (1990), 3343.

[8] T.L. Barklow: "Using $e^+e^- \rightarrow \nu\bar{\nu}t\bar{t}$ to probe strong EW symmetry breaking at the NLC", report from the Proceedings of the 1996 DPF/DPB Summer Study, Snowmass, Colorado, June 25 – July 12, 1996.

[9] M. Gintner, S. Godfrey: contribution to the Proceedings of the 1996 DPF/DPB Summer Study, Snowmass, Colorado, June 25 – July 12, 1996, `[hep-ph/9612342]`.

[10] F. Larios, C.-P. Yuan: *Phys. Rev. D* **55** (1997) 7218 ; F. Larios, T. Tait, C.P. Yuan: *Phys. Rev. D* **57** (1998) 3106

[11] M. Gintner, I. Melo: *contribution to the Proceedings of the 13 th Conference of the Slovak and Czech physicists*, Zvolen, Slovakia, Aug 1999

[12] T. Han, Y.J. Kim, A. Likhoded, G. Valencia: `[hep-ph/0005306]`

[13] S. Weinberg: *Phys. Rev.* **166** (1968) 1568

[14] M. Bando, T. Kugo, K. Yamawaki: *Phys. Rep.* **164** (1988) 217

[15] R. Casalbuoni et al.: *Phys. Lett. B* **155** (1985) 95 ; D. Dominici: *Riv. Nuovo Cim.* **20** (1997) 1

[16] Altarelli et al.: *Int. J. Mod. Phys. A* **13** (1998) 1031

[17] R. Casalbuoni et al.Phys. Lett. B2581991161

[18] F. Larios, M.A. Pérez, C.-P. Yuan: *Phys. Lett. B* **457** (1999) 334

[19] S. Dawson: *Nucl. Phys. B* **249** (1985) 42

[20] R. Barbieri, A. Strumia: *Phys. Lett. B* **462** (1999) 144